Received: 30 March 2020 | Revised: 23 November 2020 | Accepted: 25 November 2020

DOI: 10.1002/esp.5046

RESEARCH ARTICLE

ESPL WILEY

Modelling of sediment supply from torrent catchments in the Western Alps using the sediment contributing area (SCA) approach

Moritz Altmann[1] | Florian Haas[1] | Tobias Heckmann[1] | Frédéric Liébault[2] | Michael Becht[1]

[1]Department of Physical Geography, Catholic University of Eichstätt-Ingolstadt, Eichstätt, 85072, Germany

[2]INRAE, ETNA, Université Grenoble Alpes, Grenoble, France

Correspondence
Moritz Altmann, Department of Physical Geography, Catholic University of Eichstätt-Ingolstadt, 85072, Eichstätt, Germany.
Email: MAltmann@ku.de

Abstract

The production of coarse sediment in mountain landscapes depends mainly on the type and activity of geomorphic processes and topographic and natural conditions (e.g. vegetation cover) of these catchments. The supply of sediment from these slopes to mountain streams and its subsequent transport lead to sediment connectivity, which describes the integrated coupled state of these systems. Studies from the Northern Calcareous Alps show that the size of the sediment contributing area (SCA), a subset of the drainage area that effectively delivers sediment to the channel network, can be used as a predictor of sediment delivery to mountain streams. The SCA concept is delineated on a digital elevation model (DEM) using a set of rules related to the steepness and length of slopes directly adjacent to the channel network, the gradient of the latter and the vegetation cover. The present study investigates the applicability of this concept to the Western Alps to identify geomorphologically active areas and to estimate mean annual sediment yield (SY) in mainly debris-flow-prone catchments. We use a statistical approach that shows a parameter optimisation and a linear regression of SY on SCA extent. We use a dataset of ~25 years of assessed coarse sediment accumulation in 35 sediment retention basins. In the investigated catchments, sediment transport is governed by several factors, mainly by the extent of vegetation-free areas with a minimum slope of 23° that is coupled to the channel network with a very low gradient of the latter. With our improved framework, we can show that the SCA approach can be applied to catchments that are widely distributed, in a large spatial scale (hectare area) and very heterogeneous in their properties. In general, the investigated catchments show high connectivity, resulting in significant correlations between long-term average yield and the size of the SCA.

KEYWORDS

Bedload sediment yield, debris flows, French Alps, geomorphic coupling, modelling, sediment connectivity, sediment contributing area, sediment supply, vegetation

1 | INTRODUCTION

The supply of sediment from slopes to mountain streams by hillslope processes and its subsequent bedload transfer to the basin outlet represent an essential part of sediment cascades in alpine areas (Fryirs, 2013; Walling, 1983). Especially due to their topography, natural conditions and glacial inheritance, these areas have a high potential of sediment delivery caused by hydrological and geomorphological processes, which are difficult to describe due to their complexity and dependence on local conditions (Becht, 1995; Becht et al., 2003; Bishop & Shroder, 2004; Rathjens, 1982). The production of course sediment in mountain landscapes is located mainly on steep and unvegetated slopes, where rock on slopes converts to sediment through erosion and weathering (Riebe et al., 2015); For example, landslides, slope failures, rock avalanches, rockfalls and gullying are considered active sediment sources that can release large amounts of sediment. High mountain catchments with a high proportion of vegetation, on the other hand, can supply considerably less sediment, since the vegetation on these slopes retains the sediment (Evette et al., 2009; Molina et al., 2009). Thus, both the size of the sediment and the resulting sediment flux are mainly controlled by climate, vegetation and topography (Attal et al., 2015; Hales & Roering, 2005; Riebe et al., 2015; Sklar et al., 2016). Seasonal differences play a major role in the input of sediment to mountain streams and the subsequent sediment transport, by sediment bedload or debris flows processes (Meunier, 1991; Theule et al., 2012). There are limited periods, e.g. winter months, and periods affected by higher rainfall events and flash floods in spring and summer, which exceed thresholds at which sediment-supplying processes are triggered (Guzzetti et al., 2008; Haas et al., 2012; Lenzi et al., 2004, 2006; Morche et al., 2012; Nanson, 1974; Rainato et al., 2016; Turowski et al., 2011). The resulting bedload transport or debris flows are therefore a highly fluctuating temporal process. These events lead to a higher degree of connectivity and an increase in sediment transport during these events, which lead to changes in the river bed (Baewert & Morche, 2014; Haas et al., 2012; Lenzi et al., 2006; Molnar et al., 2010; Morche et al., 2012; Theule et al., 2012). Thus, both the fast hydrological response of these systems and the sediment availability on active slopes and in mountain streams lead to high bedload transport rates and debris flows in these torrent catchments. The amount of sediment discharge of a catchment thus depends on the size of the spatially distributed active sediment sources, the type and activity of the geomorphological processes, the differently distributed transport and storage forms and natural influences such as vegetation and climate.

Sediment transfer through a catchment has been conceptualised as a cascading system (Chorley & Kennedy, 1971) where geomorphic processes transfer sediment between different subsystems (e.g. landform, subcatchment or similar). Within these subsystems, different regulators govern the sediment fluxes, e.g. slope gradient and slope length (Chorley & Kennedy, 1971). Therefore, it is important to identify the sediment sources, as they form the starting points of sediment cascades for the subsequent sediment transport (Burt & Allison, 2010), which is also essentially influenced by the channel gradient (Benda & Cundy, 1990; Church, 2010; Fryirs et al., 2007b; Haas et al., 2011; Rickenmann, 2001). Such linkage of adjacent landforms, i.e. on a small spatial scale, through sediment transfer, can be seen as geomorphic coupling (Faulkner, 2008; Harvey, 2001), e.g. longitudinal, lateral and vertical coupling and different forms of decoupling, e.g. by buffers, barriers and blankets (Fryirs et al., 2007a). Coupling leads to sediment transfer; decoupling to storage (Brierley et al., 2006). These coupling states can change gradually over longer periods or radically during or after extreme events (Harvey, 2001). Sediment connectivity describes the integrated coupling state of a system at meso- and macro-scales (Faulkner, 2008; Heckmann & Schwanghart, 2013). Flow systems may have a different degree of connectivity at certain times, which Hooke (2003) classified into unconnected, partially connected, potentially connected, connected and disconnected. Another concept in geomorphology distinguishes between structural and functional connectivity. The extent to which different landscape elements are adjacent or physically connected to each other is described as structural connectivity (Turnbull et al., 2009; Wainwright et al., 2011), which thus includes the coupling of different landscape units (Brunsden, 1993). Individual or multiple geomorphological processes, instead, are described as functional connectivity, which consequently includes the process dynamics (process-based) through which e.g. sediment and water are transported between different landscape units (Fryirs, 2013; Heckmann & Vericat, 2018; Wainwright et al., 2011).

Several studies show how the drainage area can be reduced to a sediment-supplying (mobilisation and transfer) subset. For this purpose, Fryirs et al. (2007b) and Fryirs (2013) delineate the 'effective catchment area' on a digital elevation model (DEM) based on a slope threshold only, while Haas (2008), Haas et al. (2011), Sass et al. (2012) and Huber et al. (2015) use the 'sediment contributing area' (SCA) approach. This approach was developed by Haas (2008) and Haas et al. (2011) via the investigation of SY yield of hillslope channels in alpine catchments of the Northern Calcareous Alps (Germany, Bavarian). They found that there is no clear correlation between measured SY (determined by sediment traps) and the hydrological catchment size (drainage area). Therefore, Haas (2008) and Haas et al. (2011) reduced the hydrological catchment area to the sediment contributing area (SCA). This approach primarily considers the topography within the catchment area to extract those areas where sediment can be mobilised and transported towards the channel network. The SCA was delineated using a rule-based approach according to Heinimann et al. (1998), which includes the channel gradient, the slope inclination and the distance to the channel as proxies for coupling or decoupling. In addition to these three topographic parameters, Haas (2008) and Haas et al. (2011) also included the vegetation cover of the areas as a fourth parameter since vegetation-covered areas are considered to be less prone to sediment mobilisation and transport than vegetation-free areas. By applying this approach, a clear correlation (R^2 = 0.73) between the mean annual bedload SY and the size of the SCA was finally shown.

In the current study, the SCA model approach of Haas (2008) and Haas et al. (2011) was applied to another study region in the Western Alps, which is characterised by different topographic and natural conditions compared with the Northern Calcareous Alps (e.g. lithology and climate). Consequently, this study aims to (i) test the SCA model in the Western Alps and thus assess the general

transferability of the SCA model to another region. This is implemented with the approach of investigating and thus optimising the SCA delineation rules by evaluating the coefficient of determination of regression models (SY on resulting SCA size) to investigate significance and sensitivity of parameters known to govern sediment flux in steep mountain landscapes. The SCA approach by Haas (2008) and Haas et al. (2011) has been developed and tested on a comparatively small spatial scale. This is why the application to our study areas in the Western Alps also implies a test of transferability to larger spatial scales (hectare range). Independently, we (ii) test the degree to which the SCA matches an expert map of geomorphologically active areas, i.e. sediment sources that are coupled to the channel network. A further aim was to (iii) compare the results of this study in detail with previous SCA studies to show differences in the determined parameters that govern sediment flux in the respective catchments due to their different topographic and natural conditions. With our new approach, which includes a parameter optimisation and a sensitivity analysis, we also (iv) improve and further develop the SCA concept.

2 | STUDY AREA

2.1 | Geographic setting

The 35 investigated catchments belong to the French Northern Alps (Maurienne and Oisans) and Prealps (Chartreuse, Vercors-Trièves, and Bauges) and are distributed over an area of ca. 14,400-km^2, pertaining to the Isère (38), Savoie (73) and Haute-Savoie (74) administrative units (Figure 1). They cover a cumulative area of 134.2 km^2 and span a range of altitude from 235 to 3,170 m.a.s.l.

Due to the large spatial extent and the great differences of altitude, climatic conditions are highly variable in the investigated areas (Figure 2; Table 3). They are characterised by a temperate mountainous climate with main frontal rainfall regimes from the west and south (Gottardi et al., 2012). There are (i) west–east and north–south gradients of decreasing rainfall, with a maximum annual rainfall of about 2000 mm in the Chartreuse mountains and a minimum of about 750 mm in the Trièves and Maurienne valleys and (ii) a classic altitudinal gradient of decreasing temperature and increasing rainfall with elevations (Aufray et al., 2010; Gottardi et al., 2012). In addition, convective spring and summer storms predominate, which play a critical role for sediment transport in small alpine catchments (Theule et al., 2012). All 35 catchment areas are affected by such extreme precipitation events. The mean annual rainfall range for each catchment area is also listed in Table 3. The rainfall data are presented on the Hillshade of the DEM (IGN, 2013).

Most of the investigated torrents are characterised by drainage areas which are too small to maintain permanent flow all over the year. They correspond to ephemeral streams, flowing mostly during the snowmelt period and convective storms in spring and summer. No gauging stations are operating along these streams, and it is therefore not possible to document their flow regimes.

The largest part of the catchment areas is characterised by forest (see Tables 1 and 3; Copernicus Land Monitoring Service, 2012). Likewise, there is a large proportion of bare rocks or colluvium (e.g. talus slopes) and sparse vegetation as well as natural grassland. In the catchment areas, the typical vegetation composition of the Alps can be found, which is mainly governed by altitude and relief. Bare rocks and sparse vegetation are found in the upper parts and steep slopes of the study areas, while forests and grasslands are found in the lower parts (Copernicus Land Monitoring Service, 2012).

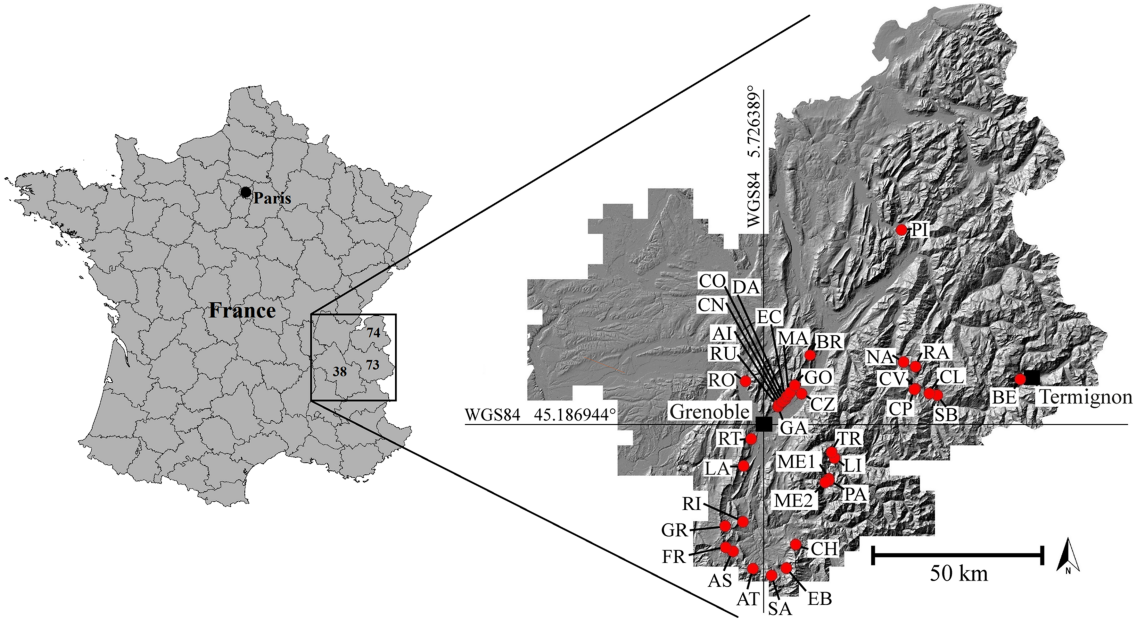

FIGURE 1 Distribution of the sediment retention basins of the torrent catchments in the French Northern Alps/Prealps used in this study (abbreviations are explained in Table 3) [Colour figure can be viewed at wileyonlinelibrary.com]

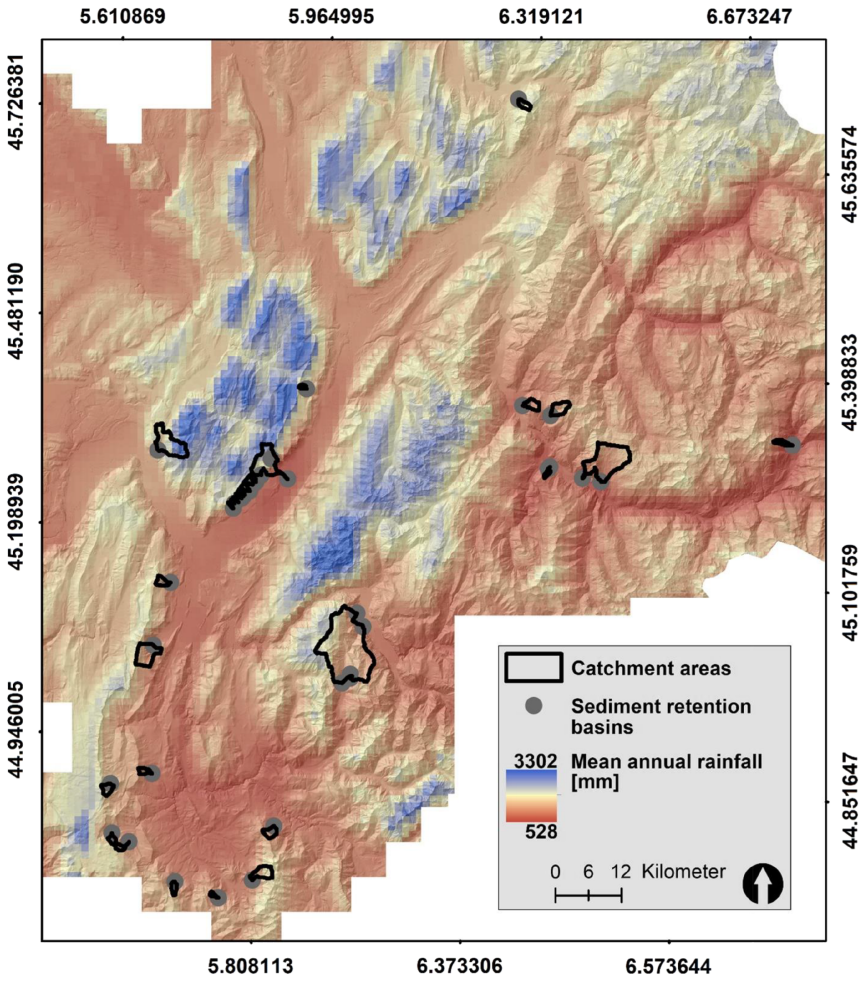

FIGURE 2 Mean annual rainfall of the French Northern Alps/Prealps (period of 1970–1999, gridded data with a resolution of 1 km from the SPAZM reanalysis, Gottardi et al. (2012)) [Colour figure can be viewed at wileyonlinelibrary.com]

TABLE 1 Landcover classes and their relative spatial extents for all catchment areas (134.2 km^2) (Copernicus Land Monitoring Service, 2012)

Landcover class	Relative extent [%]
Forest	44.3
Bare rocks/sparsely vegetated areas	26.3
Natural grasslands	19.5
Moors and heathland	3.6
Pastures	2.5
Agricultural areas	2.8
Transitional woodland-shrub	1.0

2.2 | Geological and geomorphological setting

The investigated catchments are almost all located in the sedimentary domains of the outer and inner Western Alps (32/35) (Debelmas, 1983). Only three catchments are partly entrenched into metamorphic rocks of the inner Alps: (i) the Lignarre and Treuil torrents in the Oisans geological unit, which both include steep rocky hillslopes cut into amphibolite sheets from the outer crystalline belt; and (ii) the Bey torrent in the upper Maurienne valley, partly cut into schists from the Briançonnais basement. Catchments from the Chartreuse, Vercors-Trièves and Bauges geological units are exclusively composed of alternating layers of marls and limestones of Jurassic and Cretaceous ages, typical of the Northern French Prealps. The most active sediment sources are generally concentrated in large rocky erosion cirques cut into marls and dominated by steep limestone cliffs, locally referred to as *dérochoirs*. Those steep unvegetated eroded terrains include active gullies, shallow landslides and scree slopes. Catchments from the Trièves unit differ from the other subalpine catchments due to the presence of thick lacustrine clay deposits from the Last Glacial Maximum (LGM), which are prone to deep-seated landslides. Catchments from the Oisans unit are entrenched into highly eroded and weathered Jurassic marls and limestones, some of them found exclusively within this sedimentary domain (Merdaret, Palles), some others partly composed of metamorphic rocks (Lignarre and Treuil). Catchments from the lower part of the Maurienne unit belong to a complex sedimentary unit which has been strongly crushed between crystalline basements of the inner Alps (the Ultradauphinoise zone). They are composed of a complex assemblage of highly fractured sedimentary rocks from Triassic, Jurassic and Cenozoic periods, including flysch, schists, marls, limestones, gypsum and conglomerates. Despite the strong heterogeneity of lithological conditions across the study sites, all of them were glaciated during the LGM, and glacial imprints from this period are still playing an important role in their present-day sediment dynamics. Due to the variable lithology, differences in erosion susceptibility and intensity can be expected between the study areas; the overall dominant lithology, however, is weathered limestones and marls. The topography and natural conditions of these catchment areas make them susceptible to geomorphological and hydrological

processes with high sediment activity and dynamics. In particular, the slopes in the upper parts of the catchment areas are steep (reaching mean gradients of 47° in some areas) and unvegetated, which makes them particularly prone to weathering and erosion. This is reflected today in a high runoff rate and numerous processes such as rock falls or debris flows.

3 | METHODS AND DATA

3.1 | Methods

3.1.1 | Delineation of the sediment contributing area (SCA)

The SCA approach consists of the following steps. The thresholds were set by Haas (2008) and Haas et al. (2011) in their study for the Northern Calcareous Alps (Germany, Bavarian), based on literature and field experience:

The delineation of the SCA requires a raster representation of the channel network that is consistent with the DEM, which means that the channel network cannot be taken from topographical maps but needs to be derived from the DEM, starting from manually or automatically mapped initiation cells. During a pre-processing step, sinks of the DEM were filled using the algorithm of Wang and Liu (2006). Like Haas (2008) and Haas et al. (2011), we chose a semi-automated approach where initiation cells were selected using the CIT index (channel initiation threshold; Montgomery and Dietrich (1989); Montgomery and Foufoula-Georgiou (1993); Equation 1):

$$\mathrm{CIT} = As * \tan(\beta)^2,$$

where As is the specific catchment area size [m^2m^{-1}] and β is the slope [°] ($\tan(\beta)$ = slope in % [m/m]). To ensure maximum consistency of the derived channel network with reality, we derived 100 channel networks using different CIT thresholds and evaluated their agreement with manually mapped channels on orthophotographs. This test was carried out on a subset of the study area northeast of Grenoble. The best matching channel network was derived with a CIT value of 3,800, yielding an agreement of 70%. This threshold was then applied to all study areas except 'Les Sagnes' where we used a lower threshold (3200) to improve the consistency between modelled and mapped channels.

To implement longitudinal (dis-)connectivity, the channel network is interrupted where the channel gradient falls below a user-specified threshold (3.5° in Haas et al., 2011). Areas above these sections would not form part of the SCA. In contrast to the original work by Haas (2008) and Haas et al. (2011), we refrained from decoupling the main channels, i.e. with a channel order of six or more (Strahler, 1952), in this study. This ensures connectivity in the lower parts, where channel gradients frequently fall below the threshold, but sediment transport is facilitated by (i) high, and (ii) perennial fluvial discharge (see e.g. Figure 3e) plus (iii) debris flows. This adaptation was deemed necessary as our study areas contain higher-order channels and larger SCAs compared with those investigated by Haas (2008) and Haas et al. (2011), and as initial analyses had shown that even very low minimum channel gradient thresholds led to the decoupling of several catchments. Additionally, especially the lower reaches are affected by sinks in the DEM; when they are filled by the sink-filling algorithm, a minimum slope of 0.01° is enforced, and only very low channel gradient thresholds can keep these reaches from being decoupled by the SCA algorithm.

Only hillslopes that are (i) directly adjacent to the channels, (ii) continuously steeper than a defined slope threshold and (iii) within a certain distance from the next channel are part of the SCA. Such sections of the DEM are identified by masking the DEM so that it only contains cells where (i) the slope is higher than the user-specified 'minimum slope gradient' threshold (25° in Haas et al., 2011) and (ii) the overland flow distance to the channel network is shorter than the 'maximum distance from channel network' threshold (100 m in Haas et al., 2011). Then, the upslope contributing area is derived for each (coupled) channel cell from the masked DEM, using the D8 flow routing algorithm; the result represents the SCA.

In addition to these topographic parameters, Haas (2008) and Haas et al. (2011) considered that vegetation-covered areas are less prone to sediment mobilisation and transport than vegetation-free areas. Thus they included a vegetation-dependent weighting factor in their model: Where an orthophoto-based landcover map indicated bare soil, the weight was 1 (100%), while vegetation-covered SCA cells were counted with only 20% of their original size.

Finally, the size of the (weighted) SCA is determined by applying a flow accumulation algorithm to the SCA raster dataset. Wherever SY is known, e.g. at the site of a retention basin or sediment trap, the corresponding SCA size can be extracted and used as the independent variable in a linear regression analysis of (logarithmised) bedload yield on (logarithmised) SCA size. In the study published by Haas et al. (2011), the regression was able to account for almost 75% of the observed variance of (logarithmised) bedload yield (R^2 = 0.73). The authors concluded that this model can be used to regionalise the mean annual SY from hillslope channels to rivers for their investigated area. But they also stated that the transferability of the model to other areas has to be tested in further studies, not least because the SCA sizes in their study did not exceed 8,500 m^2.

3.1.2 | Implementation of the SCA model in this study

In this study, we try to optimise the existing SCA delineation rules under the following assumption: If the SCA is, in fact, a good predictor of SY, then the coefficient of determination of a regression model (log SY on log SCA) should be a function of the parameters used to delineate the SCA. Ideally, changing one of the parameters would cause R^2 to increase systematically until an optimum is reached and R^2 decreases again.

TABLE 2 Weighting of the different vegetation-covered and vegetation-free areas

Vegetation/landcover class	Relative extent [%]	Weighting [%]
Bare rocks and sparsely vegetated areas	~25	100 (continuously)
Areas covered by vegetation	~75	100 to 0 (11 steps)
Urban structures/production industry	<1	0 (continuously)

First, 300 parameter sets with values drawn from a uniform distribution within a reasonable range were generated and applied to generate SCA to explore the dependence of R^2 on parameter settings. The parameters and their ranges are composed as follows: (i) the minimum channel gradient threshold (termed min_channel) represents longitudinal (de-)coupling, with a value range of 0° to 15°, (ii) the minimum slope gradient threshold (termed min_slope) represents lateral or hillslope-channel (de-)coupling and has a range of 0° to 45°, and (iii) the maximum distance from channel network (termed max_dist) represents the maximum slope length supporting sediment delivery to the channel, with a value range of 25 to 500 m.

The second analysis investigates the dependence of R^2 on parameter settings (sensitivity analysis) and is divided into three parts: Starting from the 'optimal' parameter set (from the first analysis), we generated several of SCAs by changing one parameter systematically while holding the remaining two constant and computed the corresponding regression models. Finally, we additionally implemented a weighting factor according to vegetation cover as described above; vegetation-covered areas were weighted from 100% to 0% in 11 steps to reveal the sensitivity of the regression model to changes in this additional parameter (Table 2). All pre-processing and processing, as well as analyses, were performed by using SAGA GIS (Conrad et al., 2015), R (R Core Team, 2019) and RSAGA (Reudenbach, 2019).

3.2 | Data

We used the RGE ALTI 2.0 DEM provided by the IGN (2013), which corresponds to a 5 m resolution DEM available for the whole French territory, combining altimetric data from different surveying techniques (airborne LiDAR and RADAR, photogrammetric restitution using aerial photographs). Data of the mean annual SY were available for 35 sediment retention basins at the outlets of the related torrent catchments (Table 3 and Figure 3). The periodic dredging of the sediment retention basins was planned by the *Restauration des Terrains en Montagne* (RTM) services of the National Forest Office, which is responsible for maintaining the protective function of the retention basins and to remove the sediment by excavators and trucks (Peteuil, 2010). The dredging of the sediment retention basins was carried out several times a year and as soon as half of the capacity was reached. Due to the regular dredging of the sediment traps, data could be collected continuously over a longer period of about 25 years (~1983 to 2008; Peteuil, 2010), and thus the mean annual SY for every sediment trap could be derived easily. The construction form of the different sediment traps is heterogeneous and differ in particular with regard to the opening design in four main types, corresponding to a trapping efficiency gradient (from the most to the less efficient): (1) sluice dams (Table 3a, b), (2) slot dams with grids, (3) slot dams without grids and (4) check-dams filled with sediments. For a more detailed description, we refer to Jousse (2009) and Peteuil (2010). Which grain sizes are retained is different for each trap and depends strongly on the clogging probability of the flow event. If clogging occurs during a flow event, all grain sizes are retained; if no clogging occurs, only the sizes greater than the opening dimension are retained. This, in turn, is controlled by the flow competence (maximum transported size), the transport of woody debris, the shape and dimension of the retention basin and the openings of the closure dam and on the degree of trap filling before the flow event (Piton & Recking, 2015; Piton et al., 2017). Therefore, we estimate that the SY data we use for several catchments are slightly lower than the actual SY that has reached the sediment retention basins.

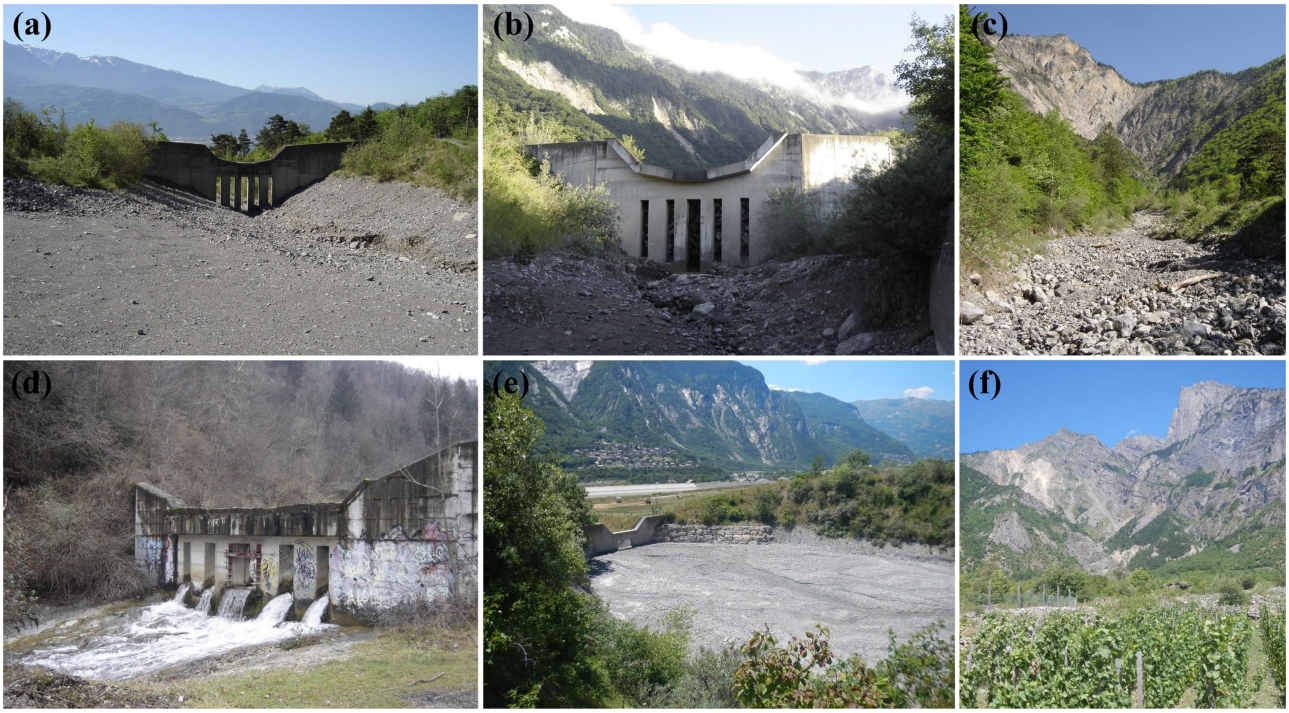

FIGURE 3 Examples of the catchment areas and sediment retention basins: (a, b) open check-dam of the sediment retention basin of the Manival Torrent (Chartreuse), (c) the main sediment production zone of the Manival Torrent (Chartreuse), (d) open check-dam of the sediment retention basin of the Roize Torrent (Chartreuse), (e) the sediment retention basin of the Claret Torrent (Maurienne) and (f) the main sediment production zone of the Claret Torrent (Maurienne) [Colour figure can be viewed at wileyonlinelibrary.com]

TABLE 3 Summary properties of the catchment areas and sediment retention basins (Jousse, 2009; Peteuil et al., 2012)

Catchment area and respective abbreviation	Drainage area [km^2]	Average annual SY [m^3]	Highest point of catchment area [m a.s.l.]	Height of sediment retention basins [m a.s.l.]	Difference between measuring height and highest point of catchment area [m]	Year of construction of retention basins
Chartreuse/Northern Prealps						
L'Aiguille (AI)	0.39	185	1,370	560	810	1970
Le Bresson (BR)	0.47	590	1,830	880	950	1989
Le Corbonne (CO)	0.79	251	1,380	510	870	1978
Le Craponoz (CZ)	8.23	614	2,060	235	1,825	1992
Le Crépon (CN)	0.41	92	1,370	540	830	1973
Le Darguil (DA)	0.90	594	1,480	570	910	1975
Les Ecorchiers (EC)	0.38	200	1,490	580	910	1987
Le Gamont (GA)	0.100	88	1,300	605	695	1993
La Gorgette (GO)	0.93	179	2,060	940	1,120	1989
Le Manival (MA)	3.72	2,304	1,740	570	1,170	1992
La Roize (RO)	11.22	772	1,845	345	1,500	1985
La Ruine (RU)	0.27	27	1,310	470	840	1972
Vercors-Trièves/Northern Prealps						
L'Archat (AT)	1.11	670	2,007	1,100	907	1991
Les Arches (AS)	1.30	3,327	1,910	1,040	870	1993
Le Chalanne (CH)	2.22	756	2,040	1,050	990	1987
L'Ebron (EB)	3.91	3,950	2,620	1,100	1,520	1990
Les Fraches (FR)	0.99	783	1,950	1,130	820	1985
La Gresse (GR)	1.89	128	2,340	258	2,082	1970
Le Lavanchon (LA)	8.23	1,337	1,975	540	1,435	1989
Le Riffol (RI)	1.02	369	1,810	850	960	1986
Le Rif Talon (RT)	1.27	565	1,870	580	1,290	1999
Les Sagnes (SA)	0.32	332	1,800	1,110	690	1998
Bauges/Northern Prealps						
Le Piézan (PI)	1.51	319	2,060	700	1,360	1983
Oisans/Northern Alps						
La Lignarre (LI)	46.12	1,404	2,860	735	2,125	1991
Le Treuil (TR)	3.96	142	2,470	790	1,680	1983
Le Merdaret/ 1,530 m (ME1)	0.91	4,750	2,435	1,530	905	1990
Le Merdaret/ 1,310 m (ME2)	3.17	11,844	2,450	1,310	1,140	1985
Les Palles (PA)	0.73	4,127	2,450	1,480	970	1988
Maurienne/Northern Alps						
Le Bey (BE)	1.33	730	3,170	1,450	1,720	1984
Le Claret (CL)	2.64	8,865	2,510	690	1,820	1991
Combe Paillarde (CP)	0.24	284	1,120	570	550	1939
Combe Varcin (CV)	0.09	225	1,265	615	650	1939
Le Nantuel (NA)	2.30	239	1,790	500	1,290	1985
La Ravoire (RA)	3.72	5,000	2,730	1,240	1,490	1991
Le St Bernard (SB)	15.58	4,039	2,825	900	1,925	1987
Total/average value	3.8	1,717	1,991	802	1,189	1983

(Continues)

TABLE 3 (Continued)

Catchment area and respective abbreviation	Sediment capacity of sediment retention basin [m^3]	Aspect	Average slope gradient [°]	Vegetation-covered area/bare rocks and sparsely vegetated area [%] (Copernicus Land Monitoring Service, 2012)	Mean annual rainfall [mm] (Gottardi et al., 2012)	Debris flows as dominant sediment transport process in catchment
Chartreuse/Northern Prealps						
L'Aiguille (AI)	3,000	SE	40.6	64/36	1,086–1,642	yes
Le Bresson (BR)	1,500	E	38.1	69/31	1,528–1,659	yes
Le Corbonne (CO)	15,000	SE	32.9	86/14	1,260–2,061	no
Le Craponoz (CZ)	NA	S	25.3	100/0	785–2,594	yes
Le Crépon (CN)	5,500	SE	43.9	78/22	1,086–1,641	yes
Le Darguil (DA)	14,000	SE	37.6	73/27	1,260–2,061	yes
Les Ecorchiers (EC)	7,000	SE	38.1	100/0	1,017–1,959	no
Le Gamont (GA)	1,000	SE	47.2	62/38	1,224–1,607	yes
La Gorgette (GO)	1,500	S	37.1	63/37	1,657–2,594	yes
Le Manival (MA)	25,000	S	36.1	84/16	1,188–2,118	no
La Roize (RO)	2,500	SW	24.7	100/0	1,383–2,692	yes
La Ruine (RU)	10,000	SE	36.3	82/18	1,224–1,607	yes
Vercors-Trièves/Northern Prealps						
L'Archat (AT)	5,000	N	37.1	67/33	1,169–1,405	no
Les Arches (AS)	2,500	E	38.7	39/61	1,170–1,615	no
Le Chalanne (CH)	2,500	NE	31.6	72/28	1,057–1,346	no
L'Ebron (EB)	100,000	W	33.5	41/59	1,127–1,677	no
Les Fraches (FR)	5,000	N	37.1	42/58	1,263–1,615	no
La Gresse (GR)	5,000	N	35.9	46/54	1,405–1,785	yes
Le Lavanchon (LA)	14,000	NE	30.4	100/0	1,159–1,675	no
Le Riffol (RI)	3,500	E	32.9	77/23	987–1,159	yes
Le Rif Talon (RT)	1,000	E	36.1	78/22	1,212–1,686	yes
Les Sagnes (SA)	300	SE	31.4	75/25	1,145–1,227	yes
Bauges/Northern Prealps						
Le Piézan (PI)	1,700	NW	34.3	100/0	1,707–1,886	yes
Oisans/Northern Alps						
La Lignarre (LI)	30,000	NE	31.7	74/26	1,139–2,114	no
Le Treuil (TR)	1,000	E	36.9	40/60	1,087–1,943	yes
Le Merdaret/1,530 m (ME1)	8,000	W	42.3	7/93	1,281–1,352	yes
Le Merdaret/1,310 m (ME2)	12,000	S	32.9	57/43	1,168–1,369	yes
Les Palles (PA)	5,000	W	38.9	5/95	1,195–1,318	yes
Maurienne/Northern Alps						
Le Bey (BE)	4,500	E	32.7	64/36	693–1,117	yes
Le Claret (CL)	23,000	SW	42.0	40/60	938–1,267	yes
Combe Paillarde (CP)	1,000	N	28.4	80/20	901–972	yes
Combe Varcin (CV)	550	N	37.5	53/47	858–972	yes
Le Nantuel (NA)	1,500	W	28.9	100/0	1,071–1,134	yes
La Ravoire (RA)	23,000	W	33.4	66/34	1,119–1,540	yes
Le St Bernard (SB)	18,000	S	24.1	67/33	806–1,503	yes
Total/average value	10,116		33.1	75/25	1,153–1,655	71% yes/29% no

For the inclusion of the vegetation cover, we used the Corine Land Cover dataset of 2012 (cell size 100 × 100 m; Copernicus Land Monitoring Service, 2012). The catchment areas of the 35 investigated sites reflect the lithological and topographical diversity of the study region which was outlined above. In addition, Table 3 shows the different properties of the catchments, their sediment retention basins and their properties relevant for this study (Jousse, 2009; Peteuil et al., 2012).

4 | RESULTS

4.1 | The size of the catchment areas

The scatterplot of log. SY against log. catchment size (Figure 4) shows a large scatter. The regression model explains 28% of the variance observed in log. mean annual SY, indicating that additional factors than catchment size governs the amount of SY.

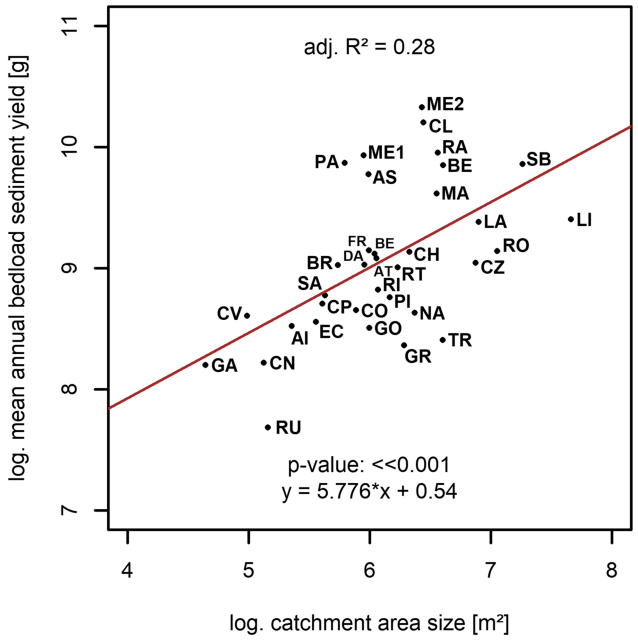

FIGURE 4 Regression of mean annual SY on catchment size [Colour figure can be viewed at wileyonlinelibrary.com]

4.2 | Sensitivity analysis of the topographic parameters

Figure 5 visualises the coefficient of determination (R^2) of the regression models of log SY on log SCA computed with 300 different parameter sets that were used to delineate the SCA. In particular, Figure 5a shows a systematic variation of R^2 with parameter settings. Model quality seems to depend predominantly on the min_channel, with good correlations between 0° and 6°; the improvement over the regression on hydrological catchment area (Figure 4) within this range shows that the SCA can be a better estimator of SY. Where the SCA is delineated with min_channel >6°, however, R^2 is systematically lower. R^2 seems to be less sensitive to variations in the min_slope parameter; however, for min_slope >33°, the coefficient of determination decreases considerably, probably because the delineated SCAs become too small. The variation of R^2 with the third parameter max_dist (Figure 5b) is much less systematic and seems to be dominated by the other parameters. The best performing parameter set (with adj. R^2 = 0.47) is marked in both plots at min_channel = 1° (including 0° in the main channels), min_slope = 23° and max_dist = 250 m.

The relative importance of the individual parameters and their systematic influence on model quality (the latter being indicated already in Figure 5) is investigated by another set of regression models where one parameter was changed systematically while the remaining two were kept constant. Figure 6 shows that the explanatory (or predictive) capacity of the regression models systematically varies with the parameter settings. In addition, the number of participating catchment areas involved in each regression was included (blue points), as certain parameter settings led to a zero SCA for some retention basins and restricted the corresponding regression analysis to the remaining ones. The min_channel threshold systematically improves the model for values between 1° and 6°, with the optimum

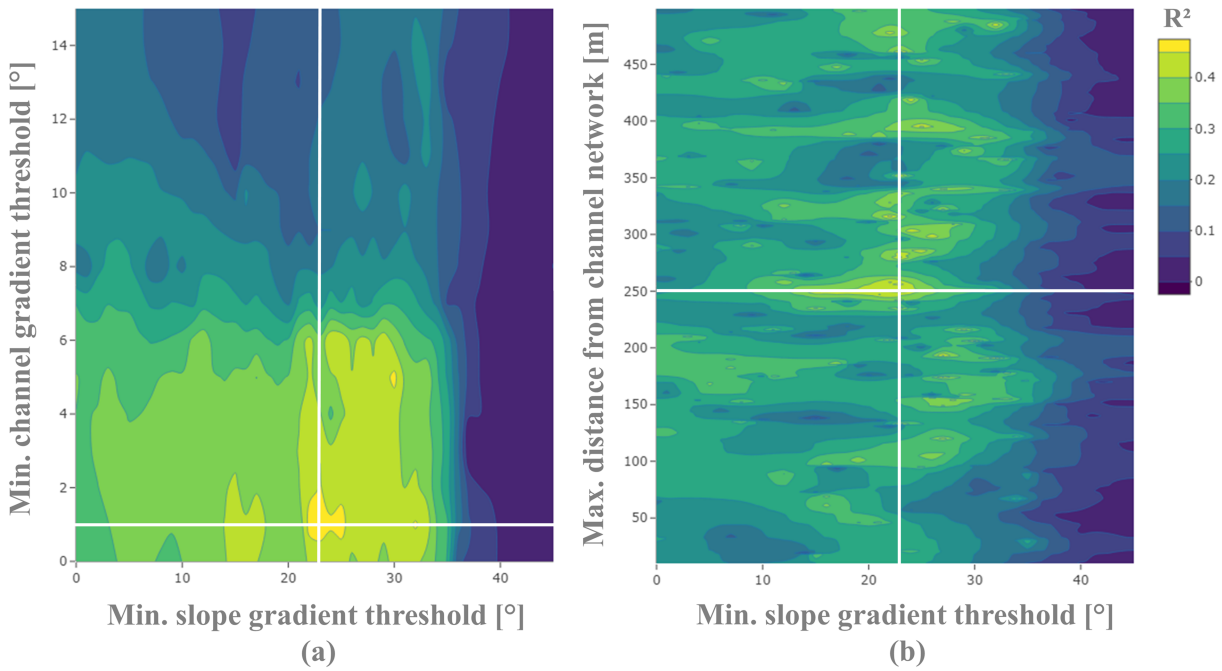

FIGURE 5 Coefficients of determination of regression models SY on SCA as a function of parameter settings used to delineate the SCA. (a) Min_channel threshold and min_slope threshold and (b) max_dist and min_slope threshold. The white cross-hairs indicate those parameter sets that led to the regression model with the highest R^2 [Colour figure can be viewed at wileyonlinelibrary.com]

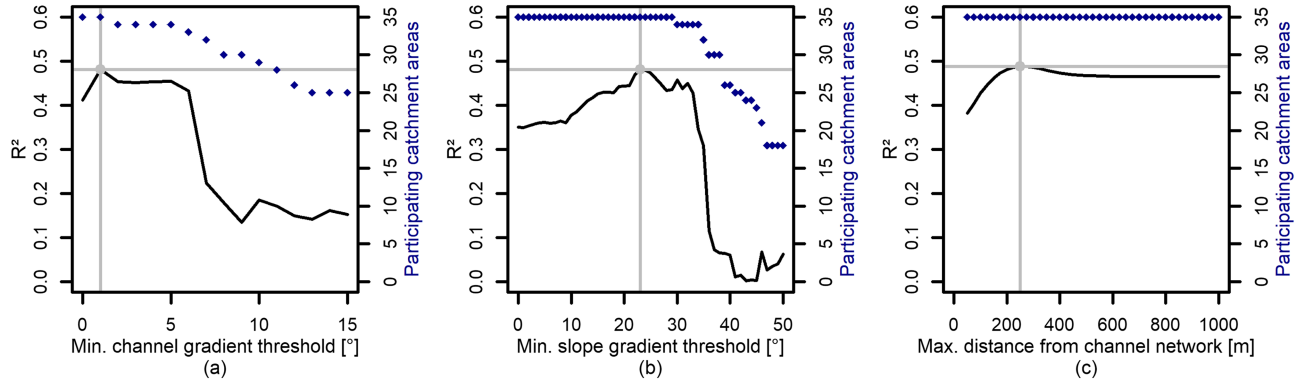

FIGURE 6 Sensitivity analysis of topographic parameters: (a) Min_channel threshold, (b) min_slope threshold and (c) max_dist [Colour figure can be viewed at wileyonlinelibrary.com]

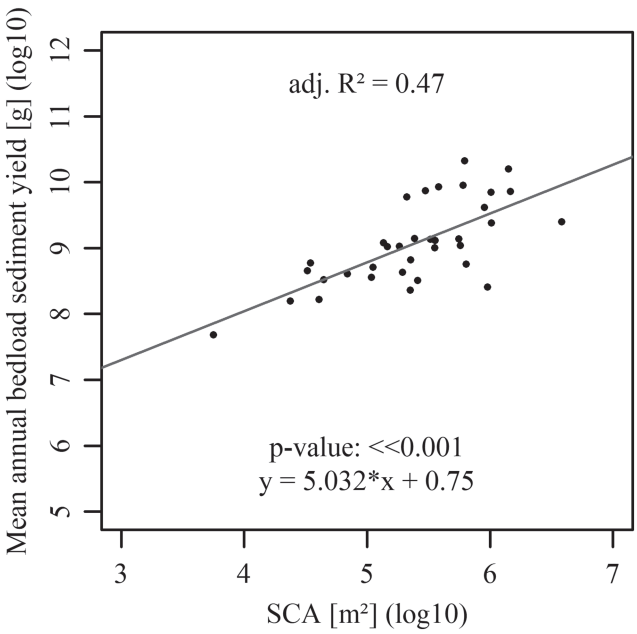

FIGURE 7 The regression model of SY on SCA size, implementing only the topographic delineation of SCA (optimised parameters: Min_channel: 1°, min_slope: 23° and max_dist: 250 m)

at 1° (highest R^2), including the main channel of 0° in the lower parts (Section 3.1.1). Higher values lead generally to a considerable decrease of R^2. This strong influence of this parameter is due to the progressive exclusion of catchment areas that become fully decoupled when the min_channel threshold increases. The min_slope threshold also systematically improves R^2 for increasing parameter settings up to an optimum at 23°; for min_slope >33°, both R^2 and the sample size decline rapidly. The parameter max_dist has its optimum between 200 and 300 m, with the highest R^2 at 250 m. Above a max. distance of 650 m, the model does not change further as the maximum possible area expansion (i.e. hillslope length) has been achieved.

The parameter optimisation ultimately led to moderate positive correlations between the size of SCA (log) and the long-term average SY (log), with the best regression model including all retention areas explaining 47% of the variance of the log-transformed SY (adj. R^2; Figure 7).

4.3 | Comparison of SCA (modelled geomorphically active areas) with mapped geomorphically active areas

Independently, the SCA delineated on the DEM was compared with a map of 'geomorphologically active' hillslope areas connected to

TABLE 4 Quantitative comparison of the SCA (modelled geomorphically active areas) with mapped geomorphically active areas. Percentage relates to the total catchment size of the retention basins

Catchment area (abbreviation)	True negative (neither mapped nor modelled active area) [%]	True positive (mapped and modelled geomorphically active area) [%]	Error of commission (modelled but not mapped) [%]	Error of omission (mapped but not modelled) [%]	Model consistent with map (true negative and true positive)/model not consistent with map (error of commission and error of omission) [%]	Kappa value
L'Aiguille (AI)	57.1	13.3	4.2	25.4	70/30	0.31
Le Bresson (BR)	NA	NA	NA	NA	NA	NA
Le Corbonne (CO)	85.1	0.2	4.5	10.2	85/15	−0.05
Le Craponoz (CZ)	90.8	1	6.3	1.9	92/8	0.15
Le Crépon (CN)	58.5	14.6	13.7	13.2	73/27	0.33
Le Darguil (DA)	66.5	3.2	15	15.3	70/30	−0.01
Les Ecorchiers (EC)	63.3	4.3	23.3	9.1	68/32	0.03

(Continues)

TABLE 4 (Continued)

Catchment area (abbreviation)	True negative (neither mapped nor modelled active area) [%]	True positive (mapped and modelled geomorphically active area) [%]	Error of commission (modelled but not mapped) [%]	Error of omission (mapped but not modelled) [%]	Model consistent with map (true negative and true positive)/model not consistent with map (error of commission and error of omission) [%]	Kappa value
Le Gamont (GA)	42.6	15.7	41.1	0.6	58/42	0.24
La Gorgette (GO)	64.6	5.6	19.3	10.5	70/30	0.1
Le Manival (MA)	71.1	5.5	18.1	5.3	77/23	0.2
La Roize (RO)	93.6	1	3.6	1.8	95/5	0.18
La Ruine (RU)	68.3	1	2	28.7	69/31	0.01
L'Archat (AT)	67.3	7.1	3.8	21.8	74/26	0.23
Les Arches (AS)	35.9	12.4	7.7	44	48/52	0.04
Le Chalanne (CH)	78.5	4.7	9.2	7.6	83/17	0.26
L'Ebron (EB)	46.3	18.4	5.3	30	65/35	0.28
Les Fraches (FR)	46.8	7.5	15	30.7	54/46	−0.05
La Gresse (GR)	60.9	7.4	4.8	26.9	68/32	0.17
Le Lavanchon (LA)	87.4	1.9	10	0.7	89/11	0.23
Le Riffol (RI)	68.6	13.1	4.9	13.4	82/18	0.47
Le Rif Talon (RT)	72	0.3	20	7.7	72/28	−0.11
Les Sagnes (SA)	72.5	0.6	6.7	20.2	73/27	−0.08
Le Piézan (PI)	56.2	2.8	39.1	1.9	59/41	0.04
La Lignarre (LI)	86	0.8	7.8	5.4	87/13	0.04
Le Treuil (TR)	69.5	2.1	16.6	11.8	72/28	−0.04
Le Merdaret/1,310 m (ME2)	54.5	13.9	7.7	23.9	68/32	0.28
Le Merdaret/1,530 m (ME1)	9.9	36.5	1.9	51.7	46/54	0.09
Les Palles (PA)	22.9	42.2	2.0	32.9	65/35	0.35
Le Bey (BE)	65.5	3.9	25.8	4.8	69/31	0.08
Le Claret (CL)	40	24.1	24	11.9	64/36	0.28
Combe Paillarde (CP)	69.2	1.1	28.8	0.9	70/30	0.04
Combe Varcin (CV)	51.9	25.1	23	0	77/23	0.38
Le Nantuel (NA)	92.4	0.1	6.9	0.6	92/8	0.02
La Ravoire (RA)	62.9	5.1	9.7	22.3	68/32	0.06
Le St Bernard (SB)	87.6	1.4	5.8	5.2	89/11	0.14
Total/Average value	79.4	3.6	8.9	8.1	83/17	0.21

the stream network. The latter were defined as sediment sources with a slope-channel coupling and were mapped in the field, from recent aerial images and orthophotos by a single operator (Jousse, 2009). We compared the mapped and modelled (SCA) maps (different way of determining the geomorphically active areas) for all catchment areas, both using quantitative metrics based on a GIS-based overlay (Table 4) and visually within six selected catchments (Figure 8). The result of the quantitative comparison shows a total compliance value of 83% and an error value of 17% (Table 4), which corresponds to a kappa value of 0.21 and fair agreement (Landis & Koch, 1977). Overall, the kappa values range from a poor (min. κ = −0.11) to a moderate agreement (max. κ = 0.47), while 50% of the catchment areas have a kappa value higher than 0.14. The visual comparison shows the agreement and types of error in six different catchment areas. The core areas, in particular, were correctly identified (true positive) by the automated approach. Errors of commission and omission are present, overall, in approximately equal proportions, which mainly occur next to the correctly identified areas. The figure also shows that the min_slope threshold used to delineate SCA seems to underestimate the extent of the mapped geomorphically active areas that start in lower parts, as the visual comparisons show (Figure 8).

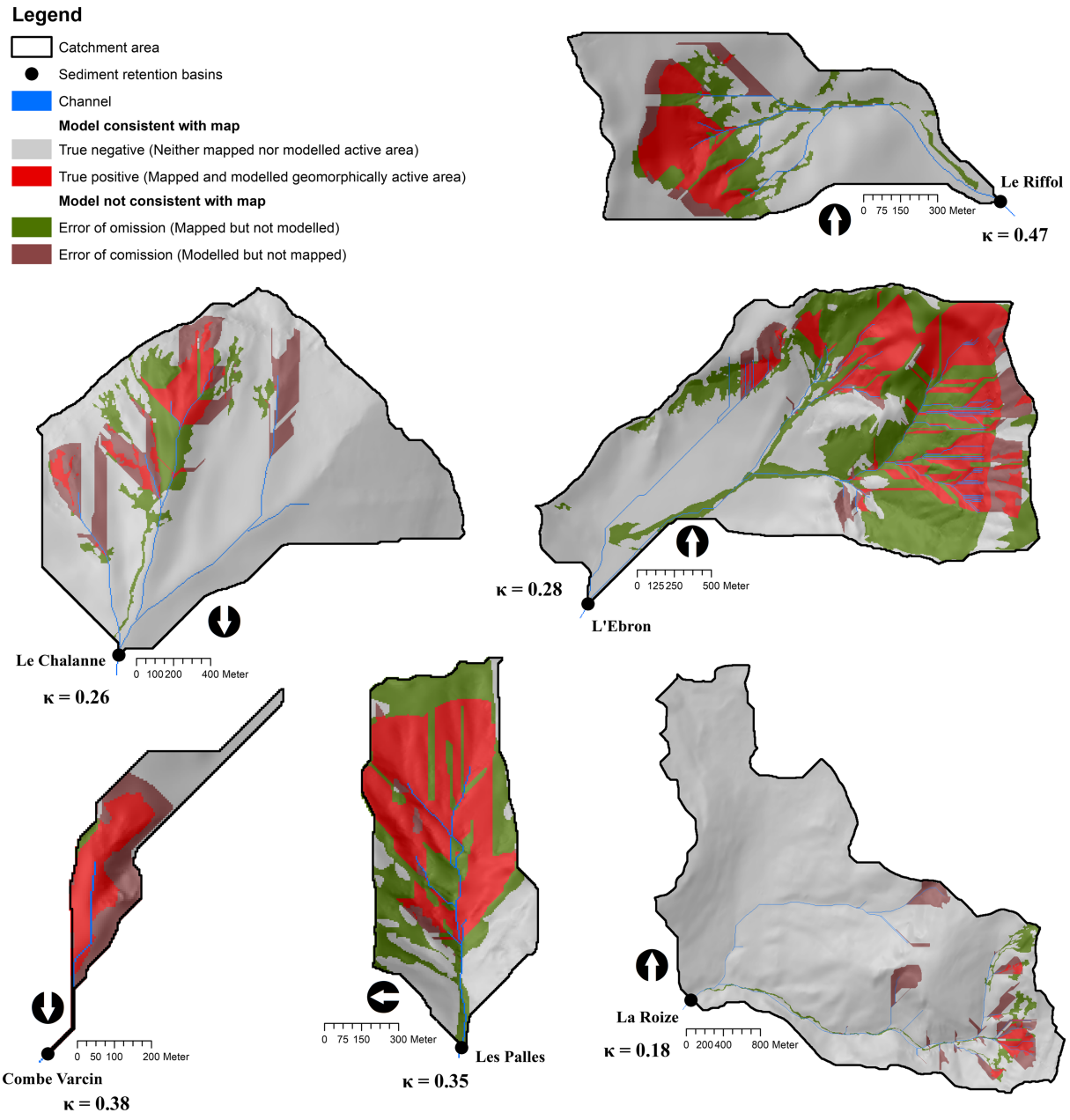

FIGURE 8 Visual comparison of SCA (modelled geomorphically active areas, only topographic parameters) with the mapped geomorphically active areas (six selected catchment areas) [Colour figure can be viewed at wileyonlinelibrary.com]

4.4 | Influence of geo-factors and homogenisation of the catchment areas involved in the model

So far, only topographical parameters were included in the analyses. In this section, we implement a weighting of SCA based on vegetation (min_channel, min_slope and max_dist are kept at their optimum values found in the previous analyses). The corresponding model shows clear improvements (Figure 9). A regression model on SCA weighted with a factor of 0.3 in vegetated areas performed best, improving the R^2 from 0.47 (adj.) to 0.53 (adj.). Both lower and higher weights led to smaller R^2. With a weighting of 0, six catchment areas were removed from the regression model, as these areas are completely covered. Figure 10 finally shows the regression line, which contains all optimised topographic parameters (min_channel: 0°/1°, min_slope: 23°, max_dist: 250 m) and the best vegetation weighting (0.3/<70%). Finally, this explains 53% of the variance of the log-transformed SY (adj. R^2; Figure 10).

In addition, the following test was performed: The catchment areas were divided into two groups depending on whether debris flows were predominant as a geomorphological process there (Table 3), and regression models were calculated separately for each of the two groups. This is based on the hypothesis that sediment transport also depends on the type and activity of geomorphic processes and that these catchments should, therefore, have a higher correlation, as the investigated groups are then more homogeneous. For this analysis, a model with these 25 catchment areas (areas with the predominant process of debris flows) was calculated. An improvement from previously 0.53 (adj. $R^2/n = 35$ ($y = 5.355x + 0.72$; $p << 0.001$)) to 0.63 (adj. $R^2/n = 25$ ($y = 4.273x + 0.95$; $p << 0.001$)) was achieved. A model was also calculated with the remaining ten

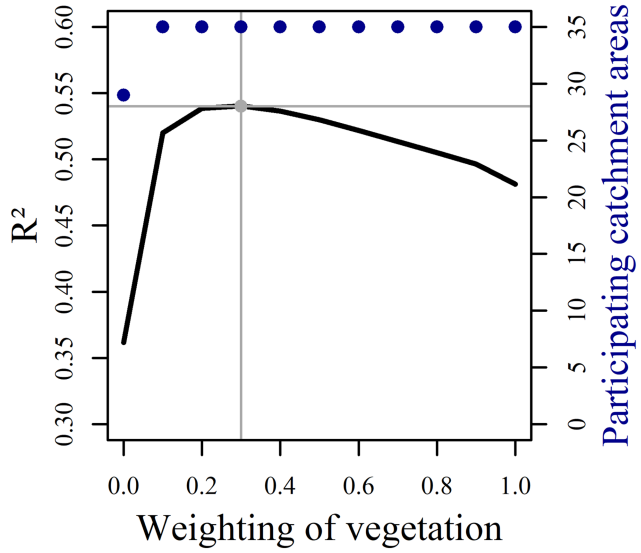

FIGURE 9 Model R^2 with implementation of a weighting factor depending on vegetation [Colour figure can be viewed at wileyonlinelibrary.com]

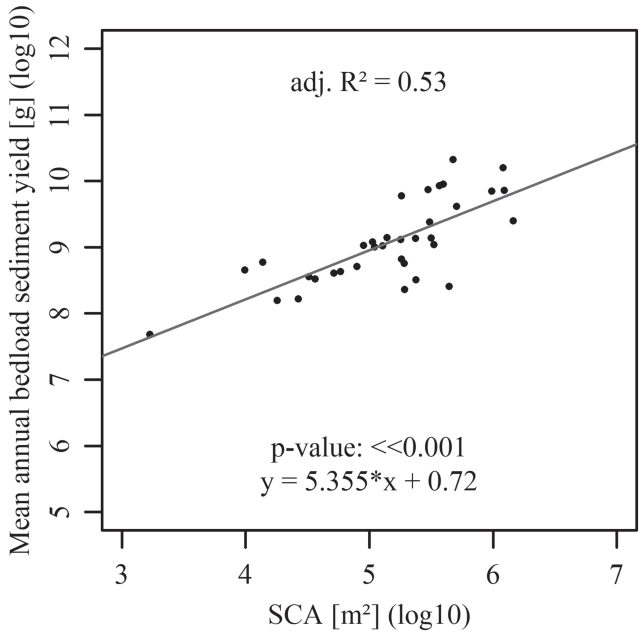

FIGURE 10 The 'final' regression model of SY on SCA size, implementing the topographic delineation of SCA and the best vegetation weighting

catchment areas (areas without the predominant process of debris flows), with a result of an R^2 of 0.50 (adj. $R^2/n = 10$ ($y = 6.484x + 0.43$; $p << 0.001$)).

5 | DISCUSSION

We delineated the sediment contributing area (SCA), a subset of the hydrological catchment area (drainage area), based on topographic parameters and landcover information (Haas, 2008; Haas et al., 2011; Huber et al., 2015; Sass et al., 2012). This is similar to the 'effective catchment area' approach of Fryirs et al. (2007b), which relies on a single slope threshold (of 2°) and a map of specific landforms. Compared with the latter approach, the rules for the delineation of SCA are only slightly more complex and do not require a geomorphological map. The advantages of the SCA approach include the low amount of required input data and the ability to implement further parameters through weighting factors. It quickly produces good results, which can be used to determine the spatial variability of mean annual sediment flux and the identification of factors under which high connectivity prevails. Nevertheless, this approach greatly simplifies the complex reality. In addition to the advantages listed above, this approach has also clear limits, such as those of the temporal scale. Since SY, the dependent variable, is computed as annual averages, this means that the regression functions do not apply to single events, let alone extreme events; strictly speaking, they only describe the average SY within the period for which average SY has been computed. Thus, it is not possible to include the consequences of seasonal differences or extreme precipitation events (external influences and their activity). Nevertheless, we assume that the measured SY is mainly attributable to these individual rainfall events. We acknowledge that, if the temporal variability of SY at the respective catchments was higher than the spatial variability between catchments, this would indicate a strong dominance of hydrometeorological drivers, and less relevance of connectivity (as modelled by SCA) in governing SY. A correlation between the area (potentially) delivering sediment to the channel network and mean annual SY only makes sense in transport-limited conditions, whereas supply limitation and considerable deposition between the sediment sources and the location where SY is measured should make correlations poorer. Considering this, the application of the SCA approach to the studied catchments in the Western Alps was not only a question of general transferability and (dis-)similarity of physical conditions, but also a question of spatial scale. The original works cited above used SY measured in sediment traps with a maximum SCA size of ca. 1 ha. The SCA study by Huber et al. (2015) yielded first indications that the relationship might hold up to SCA sizes of 1 km^2. It was conducted as part of the SedAlp project (Skolaut et al., 2015) in the Northern Calcareous Alps (50 km south of Munich/next to Bad Tölz, Germany) and used one year of data from 14 sediment traps (of the same type as those used by Haas et al., 2011). Data from two sediment retention basins with an SCA of up to 1 km^2 later increased the spatial extent of the study. Figure 11 combines our data with the previously cited SCA studies conducted in the Northern Alps (Haas, 2008; Haas et al., 2011; Huber et al., 2015). While slightly different parameter settings for the delineation of SCA and different temporal extents (see discussion below) prevent a combination of the three datasets, Figure 11 clearly shows a linear dependence of log SY on log SCA in all datasets. Considering the logarithmic data, this relationship is, in fact, that of a power law. We remark that the least-squares fitting of a linear function to logarithmic data leads to bias, so that nonlinear regression should actually be applied (Clauset et al., 2009). For reasons of comparability, however, we continued to use linear regression with logarithmised SCA and SY.

Where the SCA size of all studies overlaps (Figure 11), we observe that SY in our study is conspicuously higher than in the studies conducted in the Northern Alps; only the two largest SCAs in the study by Huber et al. (2015) have an SCA similar to the Western Alps, and they also have a similar SY. The slope of the linear regression

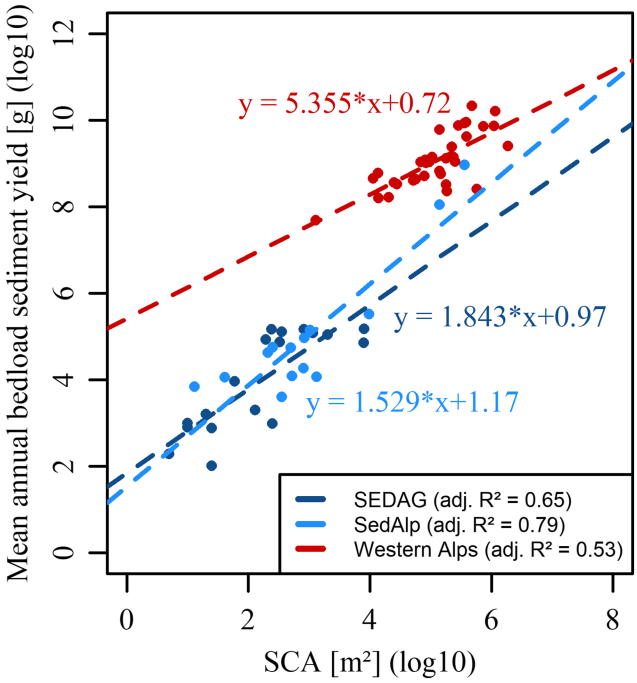

FIGURE 11 Comparison of the study in the Western Alps with studies in the Northern Calcareous Alps (Huber & Heckmann, 2015) [Colour figure can be viewed at wileyonlinelibrary.com]

functions is higher for the data from the Northern Alps, suggesting that the rate of SY increase by unit SCA appears to be lower in the Western Alps. Compared with previous SCA studies (Haas, 2008; Haas et al., 2011; Huber et al., 2015), the data in our study show greater scatter. This is probably due to the larger spatial extent and more variable characteristics of the catchment areas (e.g. lithology, climate and land cover).

Table 5 shows the properties, SCA parameter settings and results of Haas (2008) and Haas et al. (2011) for comparison with ours.

The optimum value for the coupling within the channels was found in our study with 1° in the headwaters and 0° in the main channel of all catchments (Figure 6a). This is in contrast to other SCA studies that specify or apply higher min_channel thresholds (e.g. 3.5°; Haas, 2008; Haas et al., 2011). A threshold value of 2° is also used by Fryirs et al. (2007b), but it is applied to the entire catchment area rather than to the channel gradient alone. Other studies use 2° (Heckmann & Schwanghart, 2013), 3.5° (Benda & Cundy, 1990; Wichmann, 2006) and 4° (Church, 2010) as a critical threshold for bedload transport in the channels. Beside the optimum min_channel value, our sensitivity analysis shows a similar model result up to min_channel = 6° (with 0° in the main channels), with R^2 rapidly declining when the parameter exceeds 6°. Apart from the potential influence of sinks in the DEM that were filled while imposing a minimum slope of 0.01°, we assume that two other reasons led to the low min_channel; they especially hold in the upper reaches where we did not impose a channel gradient threshold of 0°. The reasons are firstly the temporal scale and secondly the high occurrence of debris flows in the catchment areas. Previous SCA studies show higher min_channel thresholds but with shorter time scales (one to six years) (Haas, 2008; Haas et al., 2011; Huber et al., 2015), while this study covers a comparatively long time scale (~25 years), which is consistent with the observations of Harvey (2002) that spatial and temporal scales of geomorphic coupling are related in such a way that larger areas are coupled on longer time scales and vice versa. This is an indication that the transport of coarse material in higher-order channels occurs at very low gradients at least over medium time scales (in our case, decades). Furthermore, in contrast to the smaller catchment areas in the Northern Calcareous Alps, debris flows are considered as predominant process in more than 70% of the catchment areas. This is associated with a high volume of transported sediment, which can be transported over long distances (several kilometres), at high velocities and even over lower threshold values of the channel gradient (Haas, 2008; Haas et al., 2011; Theule et al., 2012).

The optimum value for the hillslope parameter min_slope is 23°. Figure 6b shows that R^2 does not decline substantially when the slope threshold is lower, thus the threshold could be lowered for better consistency with field mapping results without substantially decreasing the quality of the regression model. Other studies consistently used values close to the optimum of 23°: Heinimann et al. (1998), Heckmann and Schwanghart (2013) and Huber et al. (2015) use 30°, and Wichmann (2006), Haas (2008), Haas et al. (2011) and Sass et al. (2012) use 25°. In general, lower threshold values could be determined in the investigated catchment areas in the Western Alps compared with the other studies. Thus, the parameters min_channel and min_slope are lower in our study than in the published ones from the Northern Alpine catchments by Haas et al. (2011); this means that lower gradients are needed to sustain sediment flux. Together with the higher specific SY (i.e. larger SY per unit SCA, see Table 5) in the Northern Alps, this also indicates that sediment connectivity and erosion activity are higher in our study areas. Further reasons for this, lower gradients, higher connectivity and the higher erosion activity, could be the favourable lithology (highly erodible marls with a higher runoff coefficient), a higher proportion of sparsely vegetated areas and bare rocks and hydrometeorological factors such as higher rainfall intensities.

Our investigations showed an optimum for the max_dist at 250 m, which corresponds exactly to the value of Heinimann et al. (1998), but the R^2 of the regression models does not decline substantially for higher thresholds (Figures 5b and 6c). The very small decline beyond the optimum and the stability after max_dist exceeds the typical slope length (which is governed by lithology and climate of a landscape; see Grieve et al. (2016) and references therein) suggest that constraining the SCA by a maximum length is not needed, as the extent of the SCA on hillslopes is dominated by the min_slope parameter. Haas (2008), Haas et al. (2011) and Sass et al. (2012) set the parameter to 100 m, referring to field experience and literature, while the original work by Heinimann et al. (1998) used 250 m; however, none of these studies offer quantitative evidence justifying their choice. Due to the weak dependence of the model quality on the max_dist threshold, this parameter could be removed from the model in future applications.

Our investigations confirm that the implementation of a weighting factor of landcover improves the model, representing the role of vegetation in the prevention of erosion and as an impedance to sediment transport. The sensitivity analysis shows a consistent improvement of the model regarding the implementation of vegetation cover up to a weighting of 0.3, but even with a weighting of 0.2 or 0.4, the R^2 remained almost equally high. Lower weights

TABLE 5 Comparison of the different characteristics of the catchment areas and the threshold values determined from the study areas in the northern and Western Alps

Framework/results	Haas (2008); Haas et al. (2011) (SEDAG project)	This study
Location	Northern Calcareous Alps (Lahnenwiesgraben/Ammergebirge), Germany	Large spatial extent - > French Northern Alps (Maurienne and Oisans) and French Prealps (Chartreuse, Vercors-Trièves, and Bauges), France
Type of data acquisition (SY)	18 sediment traps (plastic troughs) in small torrents	35 sediment retention basins in torrents
Measurement period	6 years (2000 to 2005)	~25 years (~1983 to 2008)
Lithological conditions	Mainly 'Hauptdolomit' (dolomite - with high erosion resistance) and 'Plattenkalk' (limestone)	Mainly marl (highly susceptible to weathering, soft and friable) and limestone
Geomorphological and hydrological conditions	Similar geomorphological processes (e.g. debris flows, bedload transport)/ episodic channels	Similar geomorphological processes (e.g. debris flows, bedload transport)/both perennial and episodic channels
Precipitation conditions	Precipitation: 1364 mm/year (climatic station: Garmisch-Partenkirchen)	Maximum annual rainfall of about 2,000 mm in the Chartreuse mountains and a minimum of about 750 mm in the Trièves and Maurienne valleys
Proportion of covered and bare rocks/ sparsely vegetated areas [%]	92/8	75/25
Min_channel [°]	3.5	0 (lower parts)/1 (upper parts)
Min_slope [°]	25	23
Max_dist [m]	100	250
Weighting of vegetation	0.2 (reduction of 80%)	0.3 (reduction of 70%)
Regression line and R^2	Log SY = −1.843log SCA + 0.97 (R^2 = 0.65; p << 0.001)	Log SY = −5.355log SCA + 0.72 (R^2 = 0.53; p << 0.001)
Average catchment area size [km^2]	0.07	3.8
Average slope gradients [°]	32.4	33.1
Average SCA size (percentage of total area)	165 m^2 (0.24%)	14.84 ha (3,9%)
Average annual SY/SCA	59.8 g/m^2	20.8 kg/m^2

subsequently lead to significantly poorer regression models. The optimised value of 0.3 compared with bare rocks and sparsely vegetated areas is consistent with other studies that used a weight of 0.2 (Haas, 2008; Haas et al., 2011; Heinimann et al., 1998; Huber et al., 2015; Sass et al., 2012; Wichmann, 2006). Due to the resolution of 100 m of the vegetation data, however, minor uncertainties may occur due to the mixed pixel problem where a 100 m cell could contain both vegetated and bare DEM cells.

With a specific selection of the catchment areas included in the model (only those catchment areas where debris flows dominate as a geomorphological process), we can show that this leads to a better R^2 and a larger regression coefficient (more SY per SCA). The higher R^2 is thought to reflect the homogeneity of the debris flow catchments and the importance of a geomorphological classification when the approach is used for regionalisation on a larger spatial scale. Accordingly, we show that similar geomorphological processes (through a higher homogeneity of the data) can lead to a higher agreement and thus to a better regression of SY on SCA.

Finally, the SCAs delineated with our approach are fairly consistent (>80%; κ = 0.21/fair agreement) with the 'geomorphologically active' sediment sources mapped by an expert in the field. The comparison of the mapped and modelled geomorphically active areas also shows that the min_slope threshold used to delineate the SCA seems to underestimate the extent of the mapped geomorphically active areas starting in lower parts. As a result, we estimate this parameter to be even lower, with almost equal model quality. The κ values, however, are highly variable and very low in some catchments. It must be stated that, while the expert mapping aims at identifying 'geomorphologically active areas' i.e. sediment sources coupled to the channel network, the SCA delineates potentially contributing areas, addressing their activity only to a certain extent (e.g. via implementing the vegetation cover). Hence, we could not expect to get a complete match when comparing the two maps. We could also have attempted to optimise the parameters to reproduce the expert-mapped coupled sediment sources, either for all study areas or for each one separately, but we leave this to future investigations as the delineation of active areas was not our aim.

To summarise, the following observations indicate that the SCA, in fact, bears a relationship with sediment mobilisation, transfer and yield: First, there was a moderate correlation between log SY and log SCA, but only a weak one between log SY and the (log) hydrological

catchment. Second, the relationship between log SY and log SCA has the same functional form for three study areas that differ in terms of spatial and temporal scales and physical conditions. Third, the predictive or explanatory power of the models changes as a function of the parameter settings (regarding SCA delineation rules), which not only shows the consistency of the approach but also facilitates the identification of the optimal parameter settings. Last but not least, we found fair agreement between mapped sediment sources coupled to the channel network (mapped geomorphically active areas) and the SCA delineated with our approach. Together, these findings suggest that the SCA approach can be used to regionalise sediment delivery from hillslopes to channels and within the channel network. In general, we show that the SCA model is transferable to other regions, but parameter settings need to be adjusted when the approach is applied to a different area, which is due to the different topographic and vegetation conditions in the investigated catchments. To adjust the parameter settings, we recommend the optimisation approach proposed in this study.

6 | CONCLUSION

This study aims to investigate the significance and sensitivity of parameters known to govern sediment flux in steep mountain landscapes. For 35 catchments, mean annual sediment yield (SY) data were available that were measured over a period of about 25 years (~1983 to 2008) at sediment retention structures in the Western Alps. For this analysis, we used the sediment contributing area (SCA) approach, which is a set of simple DEM-based rules. Similar to the 'effective catchment area' concept, the SCA is a subset of the drainage area from which sediments are assumed to reach the channel and are transferred further. Three topographic factors, viz. the minimum channel gradient threshold (represents longitudinal (de-)coupling), the minimum slope gradient threshold (represents lateral (de-)coupling) and the maximum distance to the channel network (represents slope length), and one geo-factor, viz. the implementation of a weighting factor of landcover, representing the role of vegetation in the prevention of erosion and as an impedance to sediment transport, are considered. For the optimisation and the sensitivity analysis of these parameters, we investigated the coefficient of determination of regression models (log SY on log SCA). The results show the identification of sediment sources in the investigated catchments, which can be described mainly as bare rocks and sparsely vegetated areas continuously steeper than 23°, and that the further transport of sediment in the channel occurs at very low threshold values (0° main channels/1° headwaters). The results indicate that sediment flux is mainly governed by the minimum channel gradient threshold and the minimum slope gradient threshold. Furthermore, we show a significant improvement in R^2 when we weight the vegetation areas (reduction of 70%), which we were able to show by the sensitivity analysis of this parameter. Thus, we clearly show that vegetation-covered areas are less able to deliver sediment compared with vegetation-free slopes. In contrast, the results show that the maximum distance from the channel network is not necessary as a parameter for the delineation of the SCA, as it is not sensitive enough. Finally, the size of the SCA explains (or predicts) 53% of the variance observed in mean annual (log-transformed) SY (adj. $R^2 = 0.53$), which is much better than a regression of (log) SY on (log) drainage area (adj. $R^2 = 0.28$). When the analysis was limited to debris-flow-prone catchments (25 catchments), R^2 was even higher (0.63), highlighting the influence of homogeneous physical conditions on model quality. Both the minimum channel gradient threshold and the minimum slope gradient threshold parameter are lower compared with previous studies conducted in the Northern Calcareous Alps in Bavarian (Haas, 2008; Haas et al., 2011; Huber et al., 2015), indicating higher connectivity in our study areas in the French Western Alps. Moreover, SY appears to be higher, which is probably due to the differences in lithology, the higher proportion of unvegetated areas, the type and activity of geomorphic processes and the hydrometeorological regime. Finally, an optimum and a systematic dependence of R^2 on the parameter setting could be found for each parameter, albeit differing in their sensitivity. Independently, we compared our SCA with an expert map of geomorphologically active areas, i.e. hillslope areas functioning as sediment sources and coupled to the channel network. Although the expert map and the SCA describe different things, we found a fair agreement. We conclude that the SCA, delineated using only a DEM and landcover data, can be used to explain (or predict) mean annual sediment delivery and yield in catchment areas up to 10^1 km^2. This considerably expands the validity of this approach, as the study by Haas et al. (2011) had SCAs with a size of up to 1 ha only; moreover, our study areas are distributed over a comparatively large region, while previous studies were limited to single catchments. Finally, this study and the previous SCA studies show that the threshold values determined, which essentially control the transport of sediments through a catchment area, can vary considerably due to the topographic conditions and the natural geo-factors prevailing there. The parameters used to delineate the SCA should therefore always be calibrated using SY data from the corresponding study areas before applying the regression model.

CONFLICTS OF INTEREST

The authors declare that there are no conflicts of interest that could be perceived as prejudicing the impartiality of the research reported.

ACKNOWLEDGEMENTS

The ONF-RTM service of the Isère Department is acknowledged for making dredging data available for this study. Guillaume Evin (INRAE Grenoble) is acknowledged for processing SPAZM rainfall data shown in Figure 2 and Table 3. We also thank Cyril Jousse for the manual mapping of the sediment sources.

Open access funding enabled and organized by Projekt DEAL.

DATA AVAILABILITY STATEMENT

The data that support the findings of this study are available from third parties. The availability of these data, which have been used under licence for this study, is subject to restrictions. The data are available with the permission of the third party upon reasonable request to the corresponding author.

ORCID

Moritz Altmann https://orcid.org/0000-0001-7880-7785
Tobias Heckmann https://orcid.org/0000-0002-1495-4214

REFERENCES

Attal, M., Mudd, S.M., Hurst, M.D., Weinman, B., Yoo, K. & Naylor, M. (2015) Impact of change in erosion rate and landscape steepness on hillslope and fluvial sediments grain size in the Feather River basin (Sierra Nevada, California). *Earth Surface Dynamics*, 3(1), 201–222.

Aufray, A., Brisson, A., Tamburini, A., Dziak, V., Maloisel, V. & Martinoni-Lapierre, S. (2010) *Climat de la région Rhône-Alpes: Unpublished technical report*. Météo-France, DREAL Rhône-Alpes: 46.

Baewert, H. & Morche, D. (2014) Coarse sediment dynamics in a proglacial fluvial system (Fagge River, Tyrol). *Geomorphology*, 218, 88–97.

Becht, M. (1995) *Untersuchungen zur aktuellen Reliefentwicklung in alpinen Einzugsgebieten*. Germany, Munich: Geobuch-Verl.

Becht, M., Heckmann, T., Mittelsten Scheid, T. & Wichmann, V. (2003) *Relief und Prozesse im Alpenraum*. Heidelberg, Berlin: Spektrum.

Benda, L.E. & Cundy, T.W. (1990) Predicting deposition of debris flows in mountain channels. *Canadian Geotechnical Journal*, 27(4), 409–417.

Bishop, M.P. & Shroder, J.F. (Eds.) (2004) *Geographic information science and mountain geomorphology*. Berlin: Springer.

Brierley, G., Fryirs, K. & Jain, V. (2006) Landscape connectivity: the geographic basis of geomorphic applications. *Area*, 38(2), 165–174.

Brunsden, D. (1993) The persistance of landforms. *Zeitschrift für Geomorphologie Supplementband*, 93, 13–28.

Burt, T.P. & Allison, R.J. (2010) *Sediment cascades: An integrated approach*. Chichester: John Wiley & Sons Ltd.

Chorley, R.J. & Kennedy, B.A. (1971) *Physical Geography: A System Approach*. London: Prentice Hall.

Church, M. (2010) *Mountains and montane channels*. Chichester: Wiley-Blackwell.

Clauset, A., Shalizi, C.R. & Newman, M.E.J. (2009) Power-law distributions in empirical data. *SIAM Review*, 51(4), 661–703.

Conrad, O., Bechtel, B., Bock, M., Dietrich, H., Fischer, E., Gerlitz, L. *et al*. (2015) System for Automated Geoscientific Analyses (SAGA) v. 2.1.4. *Geoscientific Model Development*, 8(7), 1991–2007.

Copernicus Land Monitoring Service. (2012) *Corine Land Cover - CLC 2012*. https://land.copernicus.eu/pan-european/corine-land-cover

Debelmas, J. (1983) *Alpes du Dauphiné: Guides géologiques régionaux*. Paris: Masson.

Evette, A., Labonne, S., Rey, F., Liebault, F., Jancke, O. & Girel, J. (2009) History of bioengineering techniques for erosion control in rivers in western europe. *Environmental Management*, 43, 972–984.

Faulkner, H. (2008) Connectivity as a crucial determinant of badland morphology and evolution. *Geomorphology*, 100(1–2), 91–103.

Fryirs, K. (2013) (Dis)Connectivity in catchment sediment cascades: a fresh look at the sediment delivery problem. *Earth Surface Processes and Landforms*, 38(1), 30–46.

Fryirs, K.A., Brierley, G.J., Preston, N.J. & Kasai, M. (2007a) Buffers, barriers and blankets: The (dis)connectivity of catchment-scale sediment cascades. *Catena*, 70(1), 49–67.

Fryirs, K.A., Brierley, G.J, Preston, N.J. & Spencer, J. (2007b) Catchment-scale (dis)connectivity in sediment flux in the upper Hunter catchment, New South Wales, Australia. *Geomorphology*, 84(3–4), 297–316.

Gottardi, F., Obled, C., Gailhard, J. & Paquet, E. (2012) Statistical reanalysis of precipitation fields based on ground network data and weather patterns: Application over French mountains. *Journal of Hydrology*, 432–433, 154–167.

Grieve, S.W.D., Mudd, S.M. & Hurst, M.D. (2016) How long is a hillslope? *Earth Surface Processes and Landforms*, 41(8), 1039–1054.

Guzzetti, F., Peruccacci, S., Rossi, M. & Stark, C.P. (2008) The rainfall intensity–duration control of shallow landslides and debris flows: an update. *Landslides*, 5(1), 3–17.

Haas, F. (2008) *Fluviale Hangprozesse in alpinen Einzugsgebieten der nördlichen Kalkalpen: Quantifizierung und Modellierungsansätze*. Munich, Catholic University of Eichstätt-Ingolstadt: Doctoral thesis.

Haas, F., Heckmann, T., Wichmann, V. & Becht, M. (2011) Quantification and Modeling of Fluvial Bedload Discharge from Hillslope Channels in two Alpine Catchments (Bavarian Alps, Germany). *Zeitschrift für Geomorphologie, Supplementary Issues*, 55(3), 147–168.

Haas, F., Heckmann, T., Hilger, L. & Becht, M. (2012) Quantification and Modelling of Debris Flows in the Proglacial Area of the Gepatschferner/Austria using Ground-based LIDAR. In: Collins, A.L., Golosov, V., Horowitz, A.J., Lu, X., Stone, M., Walling, D.E. & Zhang, X. (Eds.) *Erosion and Sediment Yields in the Changing Environment: proceedings of an IAHS International Commission on Continental Erosion Symposium, held at the Institute of Mountain Hazards and Environment, CAS-Chengdu*, Vol. 356. China: IAHS publication, pp. 293–302.

Hales, T.C. & Roering, J.J. (2005) Climate-controlled variations in scree production, Southern Alps, New Zealand. *Geology*, 33(9), 701.

Harvey, A.M. (2001) Coupling between hillslopes and channels in upland fluvial systems: implications for landscape sensitivity, illustrated from the Howgill Fells, northwest England. *Catena*, 42(2–4), 225–250.

Harvey, A.M. (2002) Effective timescales of coupling within fluvial systems. *Geomorphology*, 44(3–4), 175–201.

Heckmann, T. & Schwanghart, W. (2013) Geomorphic coupling and sediment connectivity in an alpine catchment — Exploring sediment cascades using graph theory. *Geomorphology*, 182, 89–103.

Heckmann, T. & Vericat, D. (2018) Computing spatially distributed sediment delivery ratios: inferring functional sediment connectivity from repeat high-resolution digital elevation models. *Earth Surface Processes and Landforms*, 43(7), 1547–1554.

Heinimann, H., Hollenstein, K., Kienholz, H., Krummenacher, B. & Mani, P. (1998) *Methoden zur Analyse und Bewertung von Naturgefahren. Umwelt-Materialien, BUWAL - Bundesamt für Umwelt*. Bern: Wald und Landschaft.

Hooke, J. (2003) Coarse sediment connectivity in river channel systems: a conceptual framework and methodology. *Geomorphology*, 56(1–2), 79–94.

Huber, A. & Heckmann, T. (2015) Using sediment traps to estimate the annual sediment yield from hillslope channels. In: Becht, M. (Ed.) *Final Report on the SedAlp project*, unpublished. Eichstätt: Chair of Physical Geography, Catholic University of Eichstätt-Ingolstadt.

Huber, A., Heckmann, T., Haas, F. & Becht M. (2015) DEM-based scaling of bedload sediment yield in low-order torrents of the Isar catchment. In *Guidelines for Assessing Sediment Dynamics in Alpine Basins and Channel Reaches: Final Report of the SedAlp Project, Work Package 4*. SedAlp: Vienna; Annex, pp. 39–46.

IGN. (2013) *RGE ALTI version 2.0. Unpublished technical report, IGN, Paris, 38*.

Jousse, C. (2009) *Utilisation des plages de dépôts pour l'observation et la prédiction du transport solide torrentiel*. Unpublished MSc thesis: Strasbourg.

Landis, J.R. & Koch, G.G. (1977) The measurement of observer agreement for categorical data. *International Biometric Society*, 33(1), 159–174.

Lenzi, M.A., Mao, L. & Comiti, F. (2004) Magnitude-frequency analysis of bed load data in an Alpine boulder bed stream. *Water Resources Research*, 40(7).

Lenzi, M.A, Mao, L. & Comiti, F. (2006) Effective discharge for sediment transport in a mountain river: Computational approaches and geomorphic effectiveness. *Journal of Hydrology*, 326(1–4), 257–276.

Meunier, M. (1991) *Éléments d'hydraulique torrentielle*. Antony: Cemagref.

Molina, A., Govers, G., Cisneros, F. & Vanacker, V. (2009) Vegetation and topographic controls on sediment deposition and storage on gully beds in a degraded mountain area. *Earth Surface Processes and Landforms*, 34(6), 755–767.

Molnar, P., Densmore, A.L., McArdell, B.W., Turowski, J.M. & Burlando, P. (2010) Analysis of changes in the step-pool morphology and channel profile of a steep mountain stream following a large flood. *Geomorphology*, 124(1–2), 85–94.

Montgomery, D.R. & Dietrich, W.E. (1989) Source areas, drainage density, and channel initiation. *Water Resources Research*, 25(8), 1907–1918.

Montgomery, D.R. & Foufoula-Georgiou, E. (1993) Channel network source representation using digital elevation models. *Water Resources Research*, 29(12), 3925–3934.

Morche, D., Haas, F., Baewert, H., Heckmann, T., Schmidt, K-H. & Becht, M. (2012) Sediment transport in the proglacial Fagge River (Kaunertal/Austria). *IAHS-AISH Publ.* 356, 72–80.

Nanson, G.C. (1974) Bedload and suspended-load transport in a small, steep, mountain stream. *American Journal of Science*, 274(5), 471–486.

Peteuil, C. (2010) *Synthèse des données de production sédimentaire des bassins versants torrentiels des Alpes françaises*. Unpublished technical report. Grenoble, ONF-RTM38, 48.

Peteuil, C., Liébault, F. & Marco O. (2012) *Ecstrem, une approche pratique pour prédire la production sédimentaire des torrents des Alpes françaises*. In: Koboltschnig, G., Hübl, J. & Braun, J. (Eds.) *12th Congress Interpraevent 2012*. Klagenfurt: International Research Society Interpraevent, pp. 293–304.

Piton, G. & Recking, A. (2015) Design of Sediment Traps with Open Check Dams. I: Hydraulic and Deposition Processes. *Journal of Hydraulic Engineering*, 142(2), 1–16.

Piton, G., Carladous, S., Recking, A., Tacnet J.M., Liébault, F., Kuss, D. *et al*. (2017) Why do we build check dams in Alpine streams? An historical perspective from the French experience. *Earth Surface Processes and Landforms*, 42(1), 91–108.

R Core Team. (2019) *R: A language and environment for statistical computing*. R Foundation for Statistical Computing: Vienna, Austria: https://www.R-project.org/

Rainato, R., Picco, L. & Lenzi, M.A. (2016) Rio Cordon instrumented basin: Monitoring and investigation of June 2014 bedload event. In *BIOGRAFIA DI UN'IDEA: L'insegnamento di Salvatore Puglisi e l'attualità delle Sistemazioni Idraulico-Forestali*. Quaderni di Idronomia Montana 34, 265–274.

Rathjens, C. (1982) *Geographie des Hochgebirges: Der Naturraum*. Stuttgart: Teubner.

Reudenbach, C. (2019) *Introduction to RSAGA*. http://giswerk.org/doku.php?id=r:r-tutorials:rsaga. Accessed 15 October 2019.

Rickenmann, D. (2001) Comparison of bed load transport in torrents and gravel bed streams. *Water Resources Research*, 37(12), 3295–3305.

Riebe, C.S., Sklar, L.S., Lukens, C.E. & Shuster, D.L. (2015) Climate and topography control the size and flux of sediment produced on steep mountain slopes. *Proceedings of the National Academy of Sciences of the United States of America*, 112(51), 15574–15579.

Sass, O., Haas, F., Schimmer, C., Heel, M., Bremer, M., Stöger, F. & Wetzel, K.-F. (2012) Impact of forest fires on geomorphic processes in the tyrolean limestone alps. *Geografiska Annaler. Series A, Physical Geography*, 94(1), 117–133.

Sklar, L.S., Riebe, C.S., Marshall, J.A., Genetti, J., Leclere, S., Lukens, C.L. *et al*. (2016) The problem of predicting the size distribution of sediment supplied by hillslopes to rivers. *Geomorphology*, 277, 31–49.

Skolaut, C., Liébault, F., Habersack, H., Lenzi, M., Rusjan, S., Sodnik, J. *et al*. (2015) *Synthesis Report: Sediment Management in Alpine Basins (SedAlp): Integrating sediment continuum, risk mitigation and hydropower*.

Strahler, A.N. (1952) Hypsometric (area-altitude) analysis of erosional topography. *Geological Society of America Bulletin*, 63(11), 1117–1142.

Theule, J.I., Liébault, F., Loye, A., Laigle, D. & Jaboyedoff, M. (2012) Sediment budget monitoring of debris-flow and bedload transport in the Manival Torrent, SE France. *Natural Hazards and Earth System Sciences*, 12(3), 731–749.

Turnbull, L., Wainwright, J. & Brazier, R.E. (2009) Changes in hydrology and erosion over a transition from grassland to shrubland. *Hydrological Processes*, 24, 393–414.

Turowski, J.M., Badoux, A. & Rickenmann, D. (2011) Start and end of bedload transport in gravel-bed streams. *Geophysical Research Letters*, 38(4): 1–5.

Wainwright, J., Turnbull, L., Ibrahim, T.G., Lexartza-Artza, I., Thornton, S. F. & Brazier, R.E. (2011) Linking environmental régimes, space and time: Interpretations of structural and functional connectivity. *Geomorphology*, 126(3–4), 387–404.

Walling, D.E. (1983) The sediment delivery problem. *Journal of Hydrology*, 65(1–3), 209–237.

Wang, L. & Liu, H. (2006) An efficient method for identifying and filling surface depressions in digital elevation models for hydrologic analysis and modelling. *International Journal of Geographical Information Science*, 20(2), 193–213.

Wichmann, V. (2006) *Modellierung geomorphologischer Prozesse in einem alpinen Einzugsgebiet: Abgrenzung und Klassifizierung der Wirkungsräume von Sturzprozessen und Muren mit einem GIS*. Doctoral thesis: Munich, Catholic University of Eichstätt-Ingolstadt.

How to cite this article: Altmann M, Haas F, Heckmann T, Liébault F, Becht M. Modelling of sediment supply from torrent catchments in the Western Alps using the sediment contributing area (SCA) approach. *Earth Surf. Process. Landforms*. 2021;46:889–906. https://doi.org/10.1002/esp.5046